Computational Biology and Chemistry 55 (2015) 1–13

Contents lists available at ScienceDirect

Computational Biology and Chemistry

journal homepage: www.elsevier.com/locate/compbiolchem

A novel quantitative model of cell cycle progression based on cyclin-dependent kinases activity and population balances

Massimo Pisu [a], Alessandro Concas [a], Giacomo Cao [a,b,*]

[a] CRS4 (Center for Advanced Studies, Research and Development in Sardinia), Località Piscinamanna, Edificio 1, 09010 Pula, Cagliari, Italy
[b] Dipartimento di Ingegneria Meccanica, Chimica e Materiali, Università degli Studi di Cagliari, Piazza d'Armi, 09123 Cagliari, Italy

ARTICLE INFO

Article history:
Received 28 July 2014
Received in revised form 29 December 2014
Accepted 1 January 2015
Available online 3 January 2015

Keywords:
Population balance
Cell cycle
Modeling
Bioreactions
Kinetic parameters
Tissue cell culture

ABSTRACT

Cell cycle regulates proliferative cell capacity under normal or pathologic conditions, and in general it governs all *in vivo*/*in vitro* cell growth and proliferation processes. Mathematical simulation by means of reliable and predictive models represents an important tool to interpret experiment results, to facilitate the definition of the optimal operating conditions for *in vitro* cultivation, or to predict the effect of a specific drug in normal/pathologic mammalian cells. Along these lines, a novel model of cell cycle progression is proposed in this work. Specifically, it is based on a population balance (PB) approach that allows one to quantitatively describe cell cycle progression through the different phases experienced by each cell of the entire population during its own life. The transition between two consecutive cell cycle phases is simulated by taking advantage of the biochemical kinetic model developed by Gérard and Goldbeter (2009) which involves cyclin-dependent kinases (CDKs) whose regulation is achieved through a variety of mechanisms that include association with cyclins and protein inhibitors, phosphorylation–dephosphorylation, and cyclin synthesis or degradation. This biochemical model properly describes the entire cell cycle of mammalian cells by maintaining a sufficient level of detail useful to identify check point for transition and to estimate phase duration required by PB. Specific examples are discussed to illustrate the ability of the proposed model to simulate the effect of drugs for *in vitro* trials of interest in oncology, regenerative medicine and tissue engineering.

1. Introduction

A comprehensive understanding of the mechanisms involved in cell cycle of mammalian cells is a scientific challenge of fundamental interest and practical consequence (Nurse, 2000; Morgan, 2007). In a typical schematization of the cell cycle (cf. Fig. 1), a post-mitotic cell starts from a G1 phase, during which it grows due to biosynthetic activities and cytoplasmic organelles are replicated. Subsequently, when the G1 phase is completed, the cell enters S phase where DNA is duplicated. At the end of this process cell reaches the second phase (G2) where proteins and other cellular components needed for cell division are synthesized. Finally, cell enters M phase (mitosis) where it divides into two daughter cells. If a cell, for any reason, leaves the cell cycle, it becomes quiescent/senescent, thus reaching a resting phase called G0. Studies and findings on cell cycle mechanism, undoubtedly, have an important impact in medical science and clinical practice. A deep knowledge of cell cycle and its complex biochemical pathway may give rise to interesting investigations in oncology, toxicology, gene therapy and regenerative medicine. In addition, cell cycle is the crucial process that regulates cell growth and its proliferation during *in vitro* cell cultivation. Mammalian cells are usually cultured to produce high-value biopharmaceutical products such as monoclonal antibodies and vaccines (Sidoli et al., 2006; Liu et al., 2007; Karra et al., 2010) and to synthesize *ex vivo* biological tissues through stem cells differentiation for regenerative medicine (Lanza et al., 1996), as well as to expand specialized cells for tissue engineering (Horch, 2006). For all these reasons, the cell division cycle is one of the most intensively studied biological processes, while, on the other hand, in spite of such a great effort, many questions still remain open (Tyers, 2004). As far as eukaryotic cells are concerned, several biochemical mechanisms, which regulate the cell cycle, have been identified and discussed in the literature (Stern and Nurse, 1996; Morgan, 1997; Loog and Morgan, 2005). It is well-known that cell cycle is an ordered series of events required for the faithful duplication of one mother cell

* Corresponding author at: Dipartimento di Ingegneria Meccanica, Chimica e Materiali, Università degli Studi di Cagliari, Piazza d'Armi, 09123 Cagliari, Italy. Tel.: +39 70 675 5058; fax: +39 70 675 5057.
E-mail address: giacomo.cao@dimcm.unica.it (G. Cao).

http://dx.doi.org/10.1016/j.compbiolchem.2015.01.002
1476-9271/

Nomenclature

$A_{EF}(t)$	Superficial area in the Petri dish effectively available for adhesion of proliferating cells at time t, μm^2
$A_F(t)$	Superficial area in the Petri dish available for adhesion of proliferating cells at time t, μm^2
$A_C(t)$	Superficial area in the Petri dish roofed by proliferating adherent cells at time t, μm^2
$A_{CG1}(t)$	Superficial area in the Petri dish roofed by proliferating adherent cells in G1 at time t, μm^2
A_P	Superficial area in the Petri dish, μm^2
$f(v)$	Division probability density function, $1/\mu m^3$
k_v	Proportionality constant in the expression of the rate r_v (Eq. (20)), 1/h
N	Number of total cell, dimensionless
N_0	Number of initial total cell, dimensionless
N^P	Number of total cell for the generic P phase, dimensionless
$n^P(v, \xi, t)$	2D number density distribution of cells for the generic P phase, μm^{-3}
$\overline{n}^P(v,t)$	1D number density distribution of cells for the generic P phase in the volume variable v, μm^{-3}
$\underline{n}^P(\xi,t)$	1D number density distribution of cells for the generic P phase in the age variable, ξ, dimensionless
P	Generic phase, G1, G0, S, G2, M
p	Partitioning function, μm^{-3}
q	Coefficient appearing in the symmetric beta function, dimensionless
r_v	Time rate of change of v, $\mu m^3 h^{-1}$
r_ξ	Time rate of change of ξ, h^{-1}
t	Time, h
v	Single cell volume, μm^3
v'	Mother cell volume, μm^3
v_{max}	Maximum value for cell volume, μm^3
v_{min}	Minimum value for cell volume, μm^3
w	Shape factor of the Weibull distribution function, dimensionless

Greek letters

α	Constant parameter appearing in the definition of A_{EF}, dimensionless
$\beta(q,q)$	Symmetric beta function, dimensionless
$\Gamma(q)$	Gamma function, dimensionless
Γ_v^{G1}	Rate of transition G1 → G0, h^{-1}
λ	Scale factor of the Weibull distribution function, μm^3
μ_v	Mean of bivariate normal Gaussian distribution for v variable, μm^3
μ_ξ	Mean of bivariate normal Gaussian distribution for ξ variable, dimensionless
ξ	Age, dimensionless
τ^P	Phase maturation time for transition P → P + 1, h
$\Phi(t)$	Geometric limiting factor, dimensionless
σ_v	Standard deviation of bivariate normal Gaussian distribution for v variable, μm^3
σ_ξ	Standard deviation of bivariate normal Gaussian distribution for ξ variable, dimensionless

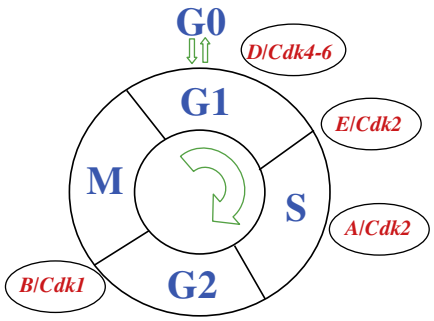

Fig. 1. The phases of a standard cell cycle. G1 (gap 1, cell grows during biosynthetic activities); S (synthesis, during this phase cell replicates DNA content); G2 (gap 2, cell grows during biosynthetic activities), M (mitosis, mother cell divides into two daughter ones); and G0 (gap 0, resting phase, cell leaves the cycle and stops to divide). The rough position in the cell cycle where the complexes D/Ckd4-6, E/Cdk2, A/Cdk2 and B/Cdk1 exert their effect is shown by oval objects.

into two daughter ones. The major role in the regulation of such events is played by specific proteins, namely cyclin-dependent kinases (CDKs). Their activity is governed by a complex network of regulatory subunits and phosphorylation/dephosphorylation events, whose precise effects on CDK conformation have been revealed by crystallographic studies (Morgan, 1997). CDKs, whose concentration levels remain almost constant throughout the cell cycle (Morgan, 2007), are small protein kinases that require association with a cyclin subunit for their activation. Cell phase progression and transition is regulated by the expression and destruction of cyclins, activating and inhibitory phosphorylation and dephosphorylation of the CDKs, as well as expression and destruction of inhibitory proteins that associate with CDKs or cyclin/CDK complexes. In the case of mammalian cells four active complexes cyclin-CDKs have been identified (Morgan, 1995, 1997, 2007; Gérard and Goldbeter, 2009), *i.e.*, D/Ckd4-6, E/Cdk2, A/Cdk2 and B/Cdk1, as reported in Fig. 1. Cell cycle is indeed a complex phenomenon, specific for each type of cells, and requires further investigations to elucidate all mechanisms which oversee the regulation of cell life and its division (Bouchoux and Uhlmann, 2011; Wittemberg, 2012). Mathematical modeling of cell cycle had a significant boost over the past two decades. In particular, two different types of the corresponding kinetic models have been developed, namely stochastic and deterministic ones. In the first approach, the mathematical models are developed to capture the fluctuations of species that characterize cellular processes. Deterministic models are instead formulated by considering suitable material balances where classical or Michaelis–Menten kinetics are accounted for. Following the stochastic approach, Tyson (1991) proposed a model for fertilized frog eggs cell cycle consisting of an alternation between S (synthesis) and M (mitosis) phase and accounting for the effect of a dimer of the protein kinase cdc2 and cyclin. The same research group, on the basis of experimental observations on yeast cell cycle, developed a more comprehensive model of eukaryotic cell cycle by considering detailed biochemistry and genetic interactions (Chen et al., 2000). This model was extended by accounting for the mitotic exit some years later (Chen et al., 2004). By means of a deterministic approach, Ciliberto et al. (2003) proposed a model to identify checkpoints that control the progression of cell cycle for budding yeast, while some years later Csikasz-Nagy et al. (2006) developed a generic model of the eukaryotic cell cycle focusing on the entire reaction network rather than on an individual phase. Gérard and Goldbeter (2009), on the basis of a deterministic approach, proposed a comprehensive biochemical kinetic model to describe the cell cycle of mammalian cells. In comparison with other models presented in the literature for this type of cells (Aguda and Tang,

1999; Qu et al., 2003; Novak and Tyson, 2004), the one proposed by Gérard and Goldbeter (2009) appears to be more detailed and complete. Results show that this approach is capable to properly simulate the behavior of the entire cell cycle and the typical oscillation experienced by cyclins and the corresponding complexes cyclin-CDK. Similar comprehensive models have been reported in the literature albeit for different type of cells (for example, Chen et al., 2004; focused on yeast cells). It is worth noting that coupling suitable cell cycle kinetic models with a mathematical tool capable of simulating cells replication and their distribution during *in vitro* cultivation may be helpful for the proper design, optimization and control of the system and in general to reduce number and costs of experiments. Models based on population balance (PB) are recognized to represent a very important theoretical tool for describing the proliferation of cells, as widely demonstrated by the growing literature addressing this topic (Liou et al., 1997; Fredrickson and Mantzaris, 2002; Pisu et al., 2003, 2004, 2006, 2007, 2008; Fadda et al., 2012a,b). PB approach, combined with proper cell cycle kinetics, may represent a potentially powerful instrument to describe, quantitatively, the evolution of an entire population during *in vitro/in vivo* cell reproduction, thus overcoming the limits of the phenomenological equations (as exponential growth, logistic, and gompertzian functions) traditionally adopted to describe the classic growth profile (sigmoidal) of total cell counts (Fadda et al., 2012a). In classic PB models the cells are seen as maturing individuals, continuously traveling along their life cycle at a specific growth rate till mitosis, which occurs at a specific transition rate (Fadda et al., 2012a). Cells in a growing population may be discriminated in terms of their own age (Faraday et al., 2001; Sherer et al., 2008) and/or size (mass or volume) (Mantzaris et al., 1999; Pisu et al., 2003, 2004, 2006, 2007, 2008) which increase along cell life cycle. In order to simplify the mathematical complexity of the model and to facilitate its experimental validation, the description of cell metabolism and its interaction with the extracellular medium may be neglected (Fadda et al., 2012a; Mancuso et al., 2009, 2010). In any case, the numerical solution of integro-partial differential equations involved in PB, remains very complex (Mantzaris et al., 1999; Ramkrishna, 2000). Furthermore, the development of classic PB models raises in general several doubts and uncertainties related to the specific selection of the proper functions needed to describe cell phase transition and growth rates. Significant changes of model output in terms of cell distributions result from different selections of such functions, being the corresponding total cell count not altered (Ramkrishna, 2000). Florian and Parker (2005) proposed an age distributed cell-cycle PB model to simulate tumor growth in the presence of chemo-therapeutic drug. Cell phases G1 and G0 were lumped into an unique "G" phase, and the same was done for G2 and M ones which have been lumped into the phase "M". Phase transition and division functions, which depend on the drug concentration for the phase S and "M", were developed as a function of a critical age which is specific for each phase. Subsequently, Liu et al. (2007) proposed a mathematical model based on a multi-staged (volume and DNA content) population balance for the simulation of *in vitro* expansion of a population of cells distributed along their cycle phases. More recently, along these lines, Fadda et al. (2012a,b); Fadda et al. (2012a,b) developed a mathematical model based on multi-staged PB with volume and DNA as internal coordinates, where different functions to describe the G1 → S and G2/M → G1 transition rates have been taken into account and a fully deterministic criterion on cell DNA content to simulate the S → G2/M transition has been considered.

In the present work, we propose a novel approach where the dynamic behavior of cell cycle phase is suitably linked to PB to simulate cellular growth and proliferation during *in vitro* cultivation occurring in a batch system (*i.e.*, monolayer adherent cells on Petri dish). In particular, in the proposed model, the transition between two consecutive cell cycle phases is assumed to be governed by the biochemical kinetics that regulates the cell cycle. Specifically, time of each phase duration (age limit of the cell in a specific phase), appearing in PB model parameters, is estimated by considering the evolution of specific biochemical reactions until check point for transition is reached. With respect to other models appearing in the literature in the present work we propose an original method to connect PB to cell cycle kinetics. Specific examples have been selected to test the ability of the proposed model to simulate the effect of a cytostatic drug and of a growth factor added during *in vitro* cell cultivation for applications in oncology or regenerative medicine/tissue engineering, respectively.

2. Mathematical modeling and numerical solution

The mathematical model proposed in this work simulates cellular growth and proliferation during *in vitro* monolayer cultivation by addressing the dynamic behavior of sub-population of cells belonging to each phase of the cell cycle. The model consists of two parts. In the first one, the model developed by Gérard and Goldbeter (2009), which describes a complex network of biochemical reactions involved in the cell cycle, is accounted for. In the second part, by means of suitable PB, the distribution of cells belonging to each cell cycle phase is described in terms of size (volume) and dimensionless maturation age for transition.

2.1. Cell cycle kinetics

The present work relies on the comprehensive kinetic model developed by Gérard and Goldbeter (2009) and characterized by 44 variables. Such model, which is focused on mammalian cells, describes a complex network of biochemical reactions involved in the cell cycle and schematically shown in Fig. 2a. The reaction network is divided into four modules each of which centered around a specific cyclin/CDK complex whose action is crucial for the progression of cell cycle (Morgan, 1995; Hochegger et al., 2008). It is apparent that cyclin D/Cdk4-6 and cyclin E/Cdk2 permit progression in G1 and elicit the G1/S transition, while cyclin A/Cdk2 ensures progression in S and the S/G2 transition, being cyclin B/Cdk1 the trigger for the G2/M transition. The growth factor (GF) activates the synthesis of cyclin D which starts the cell cycle (Gérard and Goldbeter, 2009). The model for the CDK network also incorporates regulation by the CDK inhibitor p21 (or p27) as well as the antagonistic effects of the transcription factor E2F and the tumor suppressor pRB. E2F promotes cell cycle progression by activating the synthesis of cyclins, which is repressed by pRB. Finally, the model incorporates the ATR/Chk1 DNA replication checkpoint, as shown in Fig. 2b. Cyclin E/Cdk2 activates by phosphorylation the anchor factor Cdc45, which allows DNA polymerase α to initiate replication. The kinase ATR is activated upon binding the RNA primer synthesized by DNA polymerase α. Then ATR phosphorylates, and thereby activates, the kinase Chk1 which, in turn, phosphorylates and inhibits the Cdc25 phosphatases, thus preventing the activation of Cdk2 and Cdk1, as long as DNA replication proceeds. Such a comprehensive kinetic model can properly describe cell cycle phases duration. The transition G1 → S may occur after the overcoming of G1 restriction point when the complex E/Cdk2 becomes active. The expression of DNA polymerase α indicates the exit from G1 and the starting of S-phase (maximum value of the variable DNA polymerase α). When DNA replication is completed the concentration of the enzyme DNA polymerase α rapidly diminishes and cell may exit S phase entering the next one, G2. The peak of the active complex B/Cdk1 indicates the occurrence of mitotic phase M. After cell

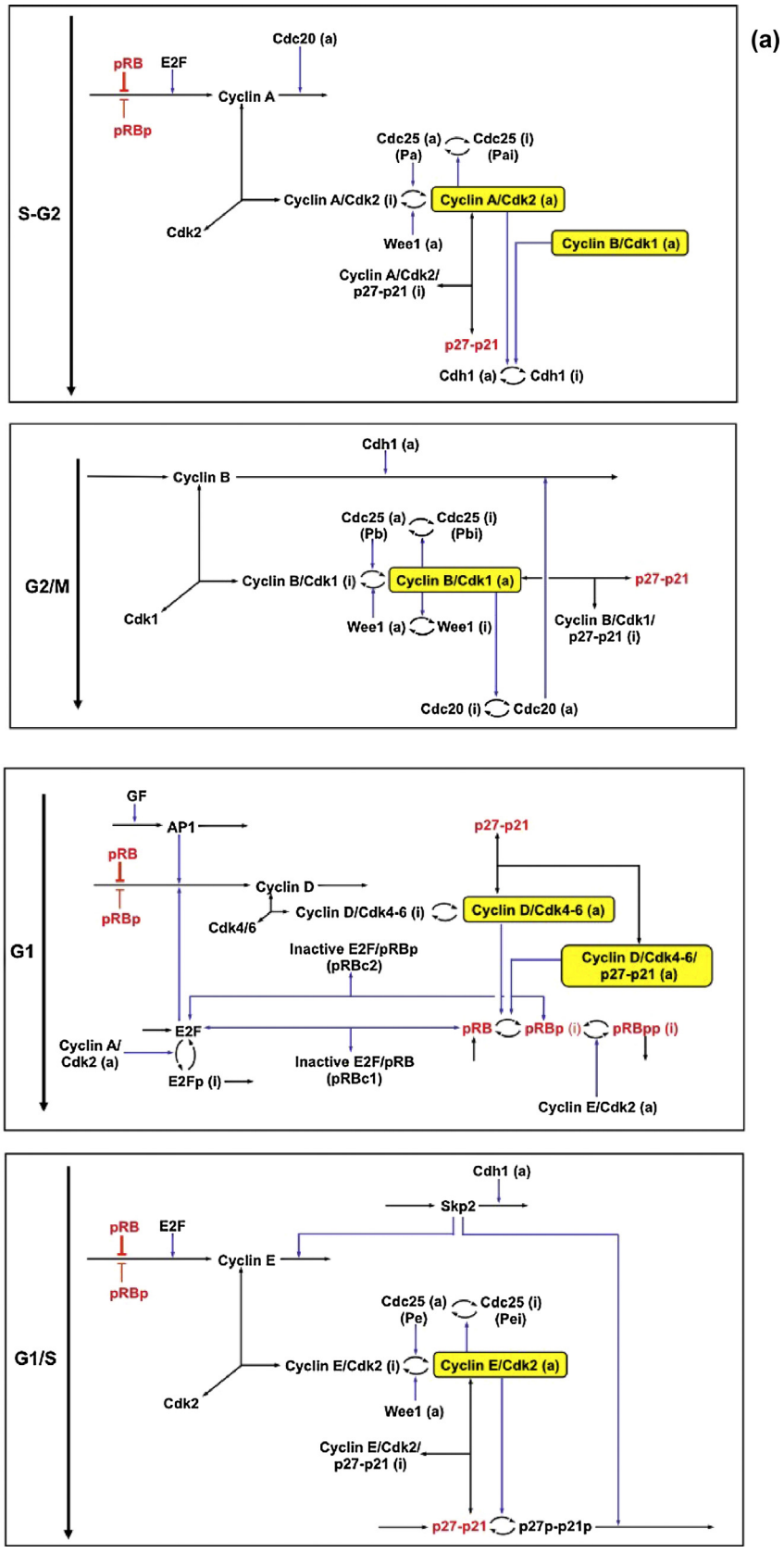

Fig. 2. Schematic representation of the biochemical kinetic network for the mammalian cell cycle which involves cyclin-dependent kinases whose regulation is achieved through a variety of mechanisms that include association with cyclins and protein inhibitors, phosphorylation–dephosphorylation, and cyclin synthesis or degradation (from Gérard and Goldbeter, 2009, 2012). (a) Representation of four kinetic modules each one centered around a specific cyclin/CDK complex, i.e, D/Ckd4-6, E/Cdk2, A/Cdk2 and B/Cdk1 (Gérard and Goldbeter, 2009, 2012) and (b) the reaction network for ATR/Chk1 DNA replication checkpoint (Gérard and Goldbeter, 2009, 2012).

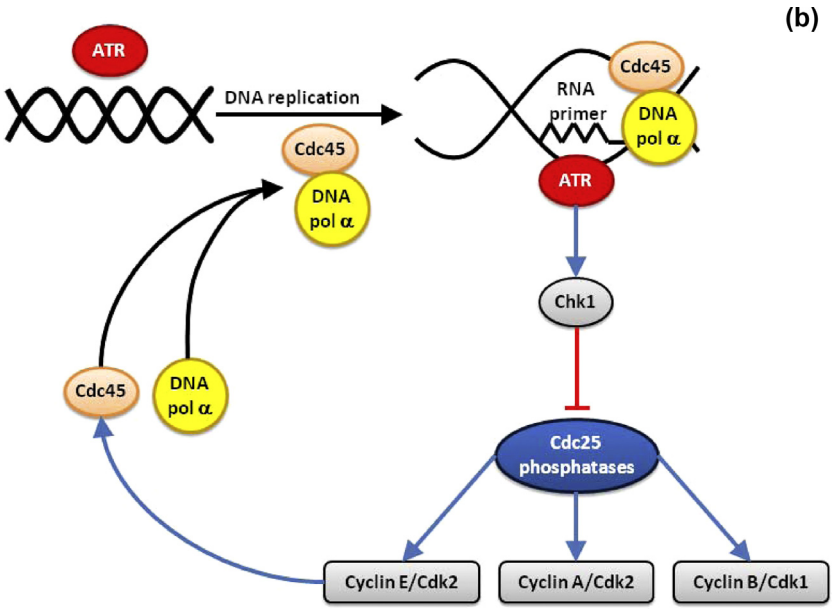

Fig. 2. (Continued)

division the concentration of complexes E/Cdk1 and A/Cdk2 drops to zero and a new cell cycle can be initiated. In the model proposed by Gérard and Goldbeter (2009), reaction rate are assumed to follow zero-th, first or second order reaction and Michaelis–Menten kinetics. For the sake of brevity all model equations, taken from the original work by Gérard and Goldbeter (2009), are not reported in this paper. The model consists of a system of 44 ordinary differential equations which is integrated as an initial value problem by means of standard numerical libraries (Gear method, IMSL). The solution of such a system provides the time duration (age) of each cell-phase necessary for transition to the next one.

2.2. Population balance

In this work we propose a mathematical model, based on PB approach, which describes cell growth and expansion by mitosis occurring in a batch system (Petri dish) while accounting for the dynamic behavior of cells belonging to the four progression stages, *i.e.*, G0, G1, S and G2/M, respectively. The latter one is a typical representation of the cell cycle where G2 and M phases are lumped together. It should be noted in passing that in principle, from a mathematical point of view, the proposed model could be easily extended to consider five phases, thus maintaining the G2 and M ones separated. With the present approach two internal coordinates are considered, namely the cell volume, v and the dimensionless age, ξ. The first one, v, theoretically ranges from zero to ∞, since cells of any positive volume may exist. Of course, this upper limit is not tractable by numerical analysis, while a zero volume should be avoided because meaningless. Actually, finite values for the lower and upper limits of cell volume ($v_{\min}$ and $v_{\max}$, respectively) may be safely chosen. The second internal coordinate, ξ, which represents a sort of age maturation index for cell in a certain phase, is particularly useful to describe the transition between two consecutive phases of the cell cycle, *i.e.*, G1 → S, S → G2/M, and G2/M → G1, respectively. ξ ranges between 0 (sub-population of cells new born in the generic phase P) and 1 (sub-population of cells that reach the check point for transition in the next generic phase P + 1).

Finally, by considering the cells spatially distributed evenly on the Petri dish and assuming negligible cell death terms, the following PB equations can be written:

$$\frac{\partial n^{G1}(v,\xi,t)}{\partial t} + \frac{\partial [r_v^{G1}(v) n^{G1}(v,\xi,t)]}{\partial v} + \frac{\partial [r_\xi^{G1} n^{G1}(v,\xi,t)]}{\partial \xi} = -[1-\Phi(t)] n^{G1}(v,\xi,t) \Gamma_v^{G1}(v) \quad (1)$$

$$\frac{\partial \overline{n}^{G0}(v,t)}{\partial t} = [1-\Phi(t)] \Gamma_v^{G1}(v) \overline{n}^{G1}(v,t) \quad (2)$$

$$\frac{\partial n^{S}(v,\xi,t)}{\partial t} + \frac{\partial [r_v^{S}(v) n^{S}(v,\xi,t)]}{\partial v} + \frac{\partial \left[r_\xi^{S} n^{S}(v,\xi,t)\right]}{\partial \xi} = 0 \quad (3)$$

$$\frac{\partial n^{G2/M}(v,\xi,t)}{\partial t} + \frac{\partial [r_v^{G2/M} n^{G2/M}(v,\xi,t)]}{\partial v} + \frac{\partial [r_\xi^{G2/M} n^{G2/M}(v,\xi,t)]}{\partial \xi} = 0 \quad (4)$$

along with the corresponding initial and boundary conditions

$$n^{G1}(v,\xi,t) = n_0^{G1}(v,\xi) \text{for} t = 0 \forall v, \xi \quad (5)$$

$$\overline{n}^{G0}(v,t) = \overline{n}_0^{G0}(v) \text{for} t = 0 \forall v \quad (6)$$

$$n^{S}(v,\xi,t) = n_0^{S}(v,\xi) \text{for} t = 0 \forall v, \xi \quad (7)$$

$$n^{G2/M}(v,\xi,t) = n_0^{G2/M}(v,\xi) \text{for} t = 0 \forall v, \xi \quad (8)$$

$$n^{G1}(v,\xi,t) = 0 \text{for} v = v_{\min} \text{and} \forall \xi, t > 0 \quad (9)$$

$$r_{\xi}^{G1} n^{G1}(v,\xi,t) = 2\int_{v}^{\infty} r_{\xi}^{G2M} n^{G2/M}(v,1,t)p(v,v')dv' \text{for} \xi = 0 \text{and} \forall v,t>0 \quad (10)$$

$$\overline{n}^{G0}(v,t) = 0 \text{for} v = v_{min} \text{and} \forall t>0 \quad (11)$$

$$n^{S}(v,\xi,t) = 0 \text{for} v = v_{min} \text{and} \forall \xi,t>0 \quad (12)$$

$$r_{\xi}^{S} n^{S}(v,\xi,t) = r_{\xi}^{G1} n^{G1}(v,1,t) \text{for} \xi = 0 \text{and} \forall v,t>0 \quad (13)$$

$$n^{G2/M}(v,\xi,t) = 0 \text{for} v = v_{min} \text{and} \forall \xi,t>0 \quad (14)$$

$$r_{\xi}^{G2/M} n^{G2/M}(v,\xi,t) = r_{\xi}^{S} n^{S}(v,1,t) \text{for} \xi = 0 \text{and} \forall v,t>0 \quad (15)$$

where $n^{P}(v,\xi,t)$ with P = G1, S, G2/M, represents the 2D number density distribution of cells, $\overline{n}^{G0}(v,t)$ is the 1D number density distribution of cell in G0 phase, and r_{ξ}^{P}, with P = G1, S, G2/M, represent the time rate of change of the internal variable v and ξ, respectively, $\Gamma_{v}^{G1}(v)$ is rate of transition G1 → G0, while $\Phi(t)$ represents the geometric limiting factor to describe cell contact inhibition (Fadda et al., 2012a). Since in the present work the transition G1 → G0 is assumed to be irreversible, it is not necessary to describe cell distribution in terms of age when considering the resting phase G0. Thus, the cells belonging to the resting phase G0 are represented by the 1D distribution $\overline{n}^{G0}(v,t)$ where the volume v in this case is the only distributed property. In Eq. (1), which represents the PB for cells in G1, the three terms of the left-hand-side describe the accumulation, the cell volume and age growth, respectively. The right-hand-side of Eq. (1) represents the removal of cells that leave the stage G1 entering the G0 phase depending on the level of confluence reached so far. Eq. (2) represents the PB for quiescent cells and describes their accumulation in phase G0 as arising from G1 cells that, due to contact inhibition, cannot cycle further to S phase. The 2D distribution for phase G1, n^{G1} is properly transformed in 1D ($\overline{n}^{G1}$ appearing in Eq. (2)) through a simple integration over the variable ξ:

$$\overline{n}^{G1}(v,t) = \int_{0}^{1} n^{G1}(v,\xi,t)d\xi \quad (16)$$

The PB for cells in S phase is reported in Eq. (3), where along with the accumulation term, two advection terms are considered in order to take into account the simultaneous growth of size (volume) and age. Analogously, the PB for cells in G2/M phase is reported in Eq. (4). The advection term containing the derivative with respect to ξ variable (last term in the right hand side of Eqs. (1)–(3) at $\xi = 1$, intrinsically accounts for the loss of cells due to the transition to the next phase.

For each phase P, corresponding to G1, S, and G2/M, respectively, the time (age) to reach the check point for transition to the next phase P + 1 is represented by τ^{P}, which corresponds to the case when $\xi = 1$ of the distributed property. In the proposed model, the transition of cells between two consecutive phases of the cell cycle is accounted for in the appropriate boundary conditions (at $\xi = 0$, Eqs. (10), (13) and (15), for G2/M → G1, G1 → S and S → G2/M, respectively). It is worth noting that the mitotic term, appearing in the boundary condition (10), is expressed in terms of unequal partitioning function since, in general, two daughter cells, obtained by a dividing mother cells, may have different dimension. The unequal partitioning distribution of mother cell into daughters, $p(v,v')$, proposed by Hatzis et al. (1995), is therefore taken into account:

$$p(v,v') = \frac{1}{\beta(q,q)}\frac{1}{v'}\left(\frac{v}{v'}\right)^{q-1}\left(1-\frac{v}{v'}\right)^{q-1} \quad (17)$$

where $\beta(q,q)$ is the symmetrical beta function:

$$\beta(q,q) = \frac{(\Gamma(q))^2}{\Gamma(2q)} \quad (18)$$

and $\Gamma(q)$ is the gamma function:

$$\Gamma(q) = \int_{0}^{+\infty} s^{q-1}e^{-s}ds. \quad (19)$$

The volume growth rates, $r_{v}^{P}(v)$ appearing in Eqs. (1)–(4) may be assumed to be linear on the basis of the references available in the literature (Tzur et al., 2009; Fadda et al., 2012a):

$$r_{v}^{P}(v) = \frac{dv}{dt} = k_{v}v \text{for P} = G1,S,G2/M. \quad (20)$$

Along these lines, it is worth noting that, the containment condition of PBs (*i.e.*, $r_{v=0}^{P} = 0$), discussed by Fredrickson and Mantzaris (2002), is automatically verified. On the other hand, the boundary conditions on v_{min} (Eqs. (9), (11), (12) and (14) result from the choice of a linear volume growth rate in order to satisfy the regularity condition (Fredrickson and Mantzaris, 2002; Fadda et al., 2012a) when $v_{min} > 0$. From the theoretical point of view, it is apparent that also the cell volume variation can be related to the cell cycle kinetics, metabolism and external stimuli. However, this important and difficult task is beyond the scope of this work and could be the subject of future investigations.

According to the proposed model, the time rate of change r_{ξ}^{P} of variable ξ should be expressed as:

$$r_{\xi}^{P} = \frac{d\xi}{dt} = \frac{1}{\tau^{P}} \text{for P} = G1,S,G2/M. \quad (21)$$

Consequently, the related advection terms in the PB above assume the classical form of age structured population balance (Himmelblau and Bischoff, 1968; Ramkrishna, 2000). Finally, the rate of transition $\Gamma_{v}^{G1}(v)$ between G1 and G0 phase is expressed as follows:

$$\Gamma_{v}^{G1}(v) = r_{v}^{G1}(v)\frac{f(v)}{1-\int_{0}^{v} f(v')dv'} \quad (22)$$

where the function $f(v)$ may be represented by a probability density function of transition volume v like the Weibull distribution, characterized by two adjustable parameters, namely w and λ (Hatzis et al., 1995):

$$f(v) = \frac{w}{\lambda^{w}}v^{w-1}\exp\left(-\left(\frac{v}{\lambda}\right)^{w}\right) \quad (23)$$

Due to space limitations, the population of adherent cells growing in a monolayer may reach the full confluence when the limited surface area of a Petri dish is completely occupied, while

proliferation stops because of contact inhibition (Fadda et al., 2012a). This phenomenon is represented by the continuous transition of cycling cells into G0 phase. Specifically, as the available surface reduces due to proliferation and size growth, a fraction of cells may leave the cycle from the stage G1 to enter the resting phase G0, where cell size growth does not occur. In the present work, although it is theoretically possible, we do not account for the back-transition G0 → G1, so that all quiescent cells remain in the resting state G0. In order to simulate contact inhibition, which progressively slows down culture expansion before reaching complete confluence in the Petri dish, a limiting factor $\Phi(t)$ appearing in the transitions G1 → G0 is introduced (Fadda et al., 2012a). Such factor is naturally related to the available superficial area between cells on the Petri dish surface, assuming that cells tend to distribute themselves on a monolayer. Specifically, if during cell cultivation, sufficient, residual surface area is still available, this limiting factor is assumed to maintain a value equal to one and irreversible transition from G1 to the resting phase G0 does not occur. On the other hand, when the free surface on the Petri dish is no more sufficient, $\Phi(t)$ is assumed to have a value less than one, so that, the transition G1 → G0 will proceed proportionally to a factor $[1-\Phi(t)]$. In this way not all the cells may complete the phase G1 (thus, reaching the value $\xi = 1$) to enter the next phase S. The limiting factor $\Phi(t)$ is calculated as proposed by Fadda et al. (2012a):

$$\Phi(t) = \begin{cases} 1 & \text{if} \quad A_{EF}(t) \geq A_{CG1}(t) \\ \left[\dfrac{A_{EF}(t)}{A_{CG1}(t)}\right] & \text{if} \quad 0 < A_{EF}(t) < A_{CG1}(t) \\ 0 & \text{if} \quad A_{EF}(t) \leq 0 \end{cases} \tag{24}$$

where

$$A_{EF}(t) = A_P(t) - \alpha A_C(t) \tag{25}$$

$$A_C(t) = (\pi)^{1/3}\left(\frac{3}{4}\right)^{2/3}\int_{v_{min}}^{\infty} v^{2/3}\left[\overline{n}^{G1}(v,t) + \overline{n}^{G0}(v,t) + \overline{n}^{S}(v,t) + \overline{n}^{G2/M}(v,t)\right]dv \tag{26}$$

$$A_{CG1}(t) = (\pi)^{1/3}\left(\frac{3}{4}\right)^{2/3}\int_{v_{min}}^{\infty} v^{2/3}\overline{n}^{G1}(v,t)dv \tag{27}$$

with

$$\overline{n}^{S}(v,t) = \int_0^1 n^{S}(v,\xi,t)d\xi \tag{28}$$

$$\overline{n}^{G2/M}(v,t) = \int_0^1 n^{G2/M}(v,\xi,t)d\xi \tag{29}$$

A_{EF} in Eq. (25) represents the effectively free surface area, A_P the Petri dish cultivation area and α a geometric shape constant. A_C, defined in Eq. (26), is the area occupied by all cells calculated as the bi-dimensional projection of a monolayer culture of spherical cells. Analogously, A_{CG1} represents the area occupied by cells belonging only to G1 phase. For details of inhibition contact modeling the interested reader should refer to Fadda et al. (2012a). It is worth noting that the contact inhibition effect plays an important role only during *in vitro* cell cultivation when confluence is approached. For *in vivo* applications this effect can be neglected.

Finally, the total cell count, $N(t)$, and the number of cells belonging to a specific phase of the cell cycle, namely $N^{G1}(t)$, $N^{G0}(t)$, $N^{S}(t)$ and $N^{G2/M}(t)$, respectively, can be expressed as follows:

$$N(t) = N^{G1}(t) + N^{G0}(t) + N^{S}(t) + N^{G2/M}(t) \tag{30}$$

$$N^{P}(t) = \int_{v_{min}}^{\infty}\int_0^1 n^{P}(v,\xi,t)dvd\xi, \text{ with P} = \text{G1, S, G2/M} \tag{31}$$

$$N^{G0}(t) = \int_{v_{min}}^{\infty}\overline{n}^{G0}(v,t)dv \tag{32}$$

Eqs. (1), (3), and (4) are partial differential equations in the independent variable t (time) and internal coordinates v and ξ, while Eq. (2), beside the variable t, is characterized by only one distributed variable, v. In this work we took advantage of the method of lines (Schiesser, 1991) which is a powerful tool for solving partial differential equations. Once their finite limits are chosen, v and ξ domains are divided using constant step size meshes, and only the partial derivatives with respect to such variables are discretized by backward finite differences. Thus, the partial differential Eqs. (1)–(4) are transformed into a system of ordinary differential equations in time, which is integrated as an initial value problem by means of standard numerical libraries (Gear method, IMSL). To numerically solve the model, 100 and 300 grid points in the v and the ξ domain, respectively are adopted. According to Sidoli et al. (2006), such a choice represents a sufficient resolution to track cell distributions when numerically solving a PB model through the method of lines. A typical computational run, performed on HP Dual CPU Intel E5440 (Quad Core) at 2800 GHz, by considering 100×300 grid points, may require more than 2 h. Actually, finer grids have been tested in this work, but they did not provide significant improvements in accuracy, while prohibitively increasing the computational time. All integrals appearing in the model equation are numerically evaluated by means of trapezoidal rule.

3. Results and discussion

In order to show the ability of the proposed modeling approach we can simulate various situations which may occur when using specific substances capable to influence cell cycle. In particular, by properly changing the relative values of its adjustable parameters, the proposed model is able either to simulate *in vitro* cytostatic effects of drugs used in oncology or the increasing in proliferation of cells induced by specific growth factors. As widely known in the literature, the duration of cell cycle phases varies considerably depending upon the type of cells under consideration (Cooper, 1997). The typical cell cycle duration of human cells which is completed within 24 h is assumed as base case. Specifically, this condition has been obtained by taking advantage of all kinetic model parameters reported by Gérard and Goldbeter (2009) except for the value of *eps* (*i.e.*, the scaling factor) which is set equal to 17.5 in the present work to ensure a cell cycle duration of 24 h. It should be noted that in the original work its value is equal to 17 which corresponds to a duration of the cell cycle of 24.7 h for the case when the rate constant of cyclin E synthesis induced by E2F, k_{ce}, was set to 0.24 h^{-1} and without coupling the model with the circadian clock. For the sake of brevity the values of model parameters and the initial concentration of all involved biochemical species, used in the simulations, are taken from t he original work by Gérard and Goldbeter (2009) and are not reported in this paper. In Fig. 3, simulation results are depicted in terms of concentration as a function of time

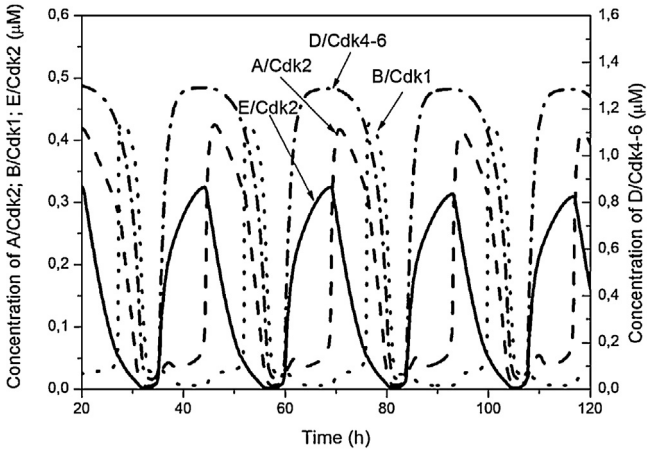

Fig. 3. Simulation results of the kinetic model in terms of the four active cyclin-CDK complexes, i.e, D/Ckd4-6, E/Cdk2, A/Cdk2 and B/Cdk1, which govern the cell cycle progression, as a function of time.

for all key cyclin-CDK active complexes, namely D/Cdk4-6, E/Cdk2, A/Cdk2 and B/Cdk1. It can be observed the typical oscillating behavior of cyclin-CDK complexes over the cell cycle which is repeated, periodically, in 24 h. Focusing on a single cycle, each phase duration τ_P, where P = G1, S, G2, M, may be calculated. In Fig. 4a, simulation results for a single cell cycle of 24 h, in terms of concentration as a function of time of active E/Cdk2, A/Cdk2 and B/Cdk1 complexes as well as DNA polymerase α are shown as base case. Starting from a cell belonging to the stage G1, the transition to the next phase S may occur when the biological check point is reached, *i.e.*, in the presence of the active complex E/Cdk2 which triggers this transition, while the concentration of DNA polymerase α reaches the maximum to sustain the DNA replication ($t = \tau^{G1} = 5.4$ h). Next, cell in S phase undergoes the transition to G2 one, when the new check point is reached. This occurs when DNA replication is completed while the concentration of DNA polymerase α starts to decrease ($t = 16$ h; $\tau^S = 10.6$ h). The subsequent cell phase transition, i.e, G2 → M, may take place when the active complex B/Cdk1 displays a peak ($t = 19$ h; $\tau^{G2} = 3$ h). Finally, cell can complete the cycle by performing the mitotic process. At the end of the cell division ($t = 24$ h; $\tau^M = 5$ h) the active complexes E/Cdk2 and A/Cdk2 concentrations drop to zero and cell restarts in G1 phase. The time of maturation for a cell belonging to the lumped phase G2/M, $\tau^{G2/M}$, necessary to undergo the transition in G1 phase can be easily computed by adding the time τ^M to τ^{G2} (*i.e.*, $\tau^{G2/M} = \tau^{G2} + \tau^M = 8$ h). Starting with this base case, it is now possible to show the ability of the proposed modeling approach in simulating various situations which may occur when using specific substances capable to influence cell cycle. Specifically, in oncologic therapies, drugs are employed to induce cytostatic effects which inhibit proliferation and cause arrests at specific cell cycle phases (Shapiro and Harper, 1999). In particular, by inhibiting CDKs activity and reducing the formation of the activated complex CDK-cyclin necessary for phosphorylation processes, cell cycle speed may be slowed down (Shapiro and Harper, 1999). This situation, for *in vitro* applications, may be suitably described by the adopted biochemical model which is characterized by a sufficient level of details to identify a possible kinetic target of a specific drug. In this case, the cytostatic effect of a drug can be simulated by properly changing one of the kinetic model parameters, *i.e.*, the basal rate of synthesis of the transcription factor E2F, being the latter one a protein which is capable to promote the cell progression by triggering the synthesis of cyclin/CDK complexes. In particular, in Fig. 4b the simulation of the cytostatic effect induced by a certain drug that increases the duration of the cell cycle is shown. All simulation

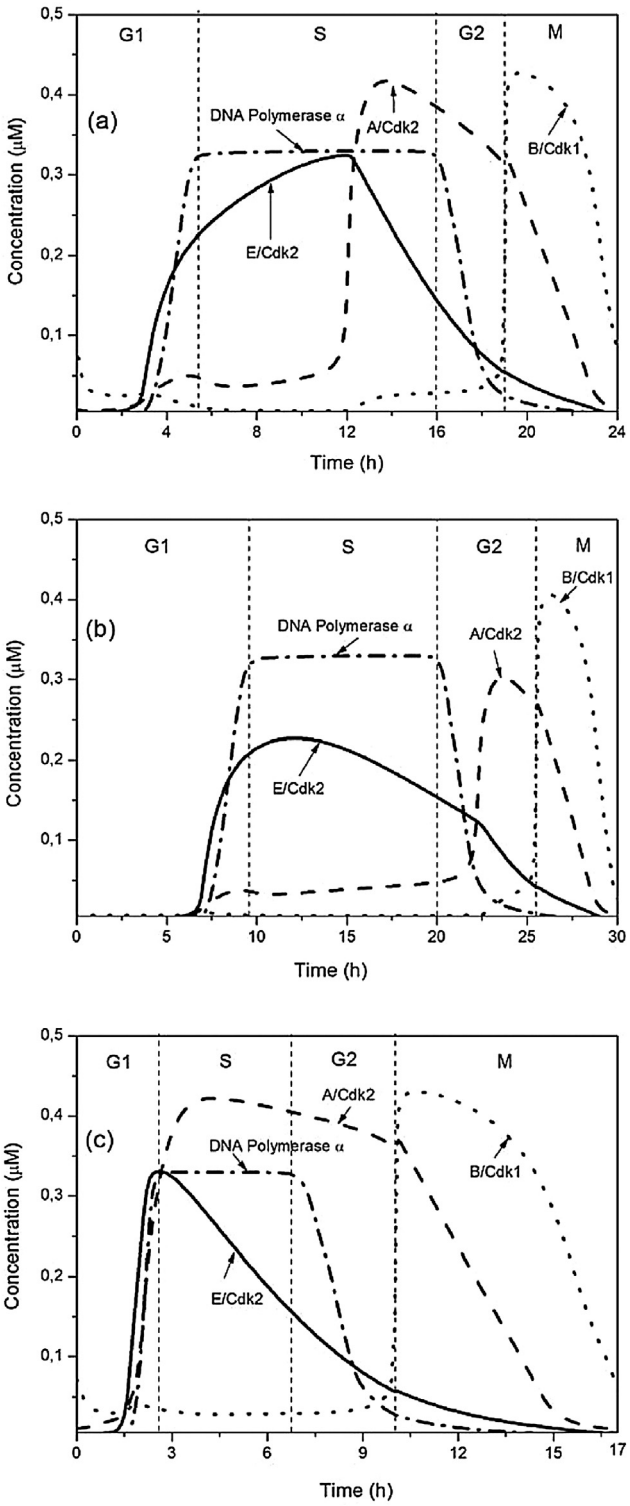

Fig. 4. Cell phase transition simulated by means of the kinetic model proposed by Gérard and Goldbeter (2009). (a) Base case with cell cycle of 24 h ($\tau^{G1} = 5.4$ h, $\tau^S = 10.6$ h, $\tau^{G2} = 3$ h, $\tau^M = 5$ h; $\tau^{G2/M} = \tau^{G2} + \tau^M = 8$ h); (b) case when a cytostatic drug is added, cell cycle of 30 h ($\tau^{G1} = 9.5$ h, $\tau^S = 10.5$ h, $\tau^{G2} = 5.5$ h, $\tau^M = 4.5$ h; $\tau^{G2/M} = \tau^{G2} + \tau^M = 10$ h); and (c) case when a substance acting as a growth factor is added, cell cycle of 17 h ($\tau^{G1} = 2.6$ h, $\tau^S = 4$ h, $\tau^{G2} = 3.4$ h, $\tau^M = 7$ h; $\tau^{G2/M} = \tau^{G2} + \tau^M = 10.4$ h).

parameters are taken from Gérard and Goldbeter (2009) except for the basal rate of synthesis of the transcription factor E2F, V_{se2f}, which is reduced from 0.15 to 0.06 μM/h. The time required to complete the cell cycle is now equal to 30 h, while the duration

of the phases is $\tau^{G1} = 9.5$ h, $\tau^{S} = 10.5$ h and $\tau^{G2/M} = \tau^{G2} + \tau^{M} = 5.5 + 4.5$ h = 10 h, respectively. In this example, as expected, the major effect is induced in the duration of G1 phase ($\tau^{G1} = 9.5$ h instead of 5.4 h as in the base case), since the inhibition of the transcription factor E2F by the drug leads to a delay in the formation of the active complex E/Cdk2 which, in turn, is necessary to trigger the transition G1 → S. This prolongation in cell cycle time leads to a reduction of the proliferative capabilities of cells (cytostasis). A stronger effect of the drug may induce the arrest of a specific cell phase and of the entire cycle. In regenerative medicine and tissue engineering, growth factors are added to increase the proliferative capacities of cells during *in vitro* cultivation (Popović and Pörtner, 2012). An acceleration of the cell cycle might be achieved by adding specific substances capable to affect the synthesis of pRB (retinoblastoma protein) which controls the inhibition of the cell cycle progression. The adopted biochemical model properly describes the hypothetical effect of specific substances on pRB kinetics and on the entire cell cycle. In Fig. 4c, the possible accelerating effect of a substance that reduces the rate of pRB synthesis is illustrated. All kinetic model parameters are taken from Gérard and Goldbeter (2009) except for the basal rate of synthesis of pRB, $V_{sprb,}$ which is reduced from 0.8 to 0.4 μM/h. In this case, the duration of entire cell cycle reduces to 17 h while the duration of the phases is $\tau^{G1} = 2.6$ h, $\tau^{S} = 4$ h and $\tau^{G2/M} = \tau^{G2} + \tau^{M} = 3.4 + 7$ h = 10.4 h, respectively. The effect of acceleration induced by acting on pRB synthesis is particularly evident for G1 and S phase whose duration is more than halved with respect to the base case ($\tau^{G1} = 2.6$ h instead of 5.4 h, and $\tau^{S} = 4$ h instead of 10.6 h, respectively).

The knowledge of each single phase duration is required by the population balance here proposed. Such parameters, namely τ^{P}, where P = G1, S, G2/M, govern the phase transition and their values can be employed to estimate the time rate of change r_{ξ}^{P} of variable ξ defined in Eq. (21) of the PB model. In the present work we considered various seeding conditions performed by means of different values of initial cell number (*i.e.*, $N_0 = 1.6 \times 10^4$; 8.0×10^4; 1.6×10^5; 3.2×10^5). The initial cell distribution for cells in G1 phase (appearing in the initial condition (5)), as a function of the variables v, and ξ, was assumed to follow the bivariate normal gaussian distribution:

$$n^{G1}(v,\xi,t=0) = n_0^{G1}(v,\xi) = \frac{N_0}{2\pi\sigma_v\sigma_\xi}\exp\left(-\frac{1}{2}\left[\frac{(v-\mu_v)^2}{\sigma_v^2} + \frac{\left(\xi-\mu_\xi\right)^2}{\sigma_\xi^2}\right]\right)$$

This expression is characterized by the mean values μ_v and μ_ξ as well as the standard deviations σ_v and σ_ξ of the variable v and ξ, respectively. No cells are assumed to pertain to the other phases (*i.e.*, $\overline{n}^{G0}(v,t=0) = \overline{n}_0^{G0}(v) = 0$; $n^{S}(v,\xi,t=0) = n_0^{S}(v,\xi) = 0$; $n^{G2/M}(v,\xi,t=0) = n_0^{G2/M}(v,\xi) = 0$ appearing in the initial conditions (6)–(8), respectively). Parameters of the bivariate gaussian function, used to describe initial distribution, are reported in Table 1 (in this simulation $\mu_\xi = 0.2$ and $\sigma_\xi = 0.01$).

In Fig. 5,the initial distributions of cells in G1 phase as a function of v (Fig. 5a) and ξ (Fig. 4b) are shown. Fig. 6 illustrates model results in terms of total counts evolution obtained at different seeding conditions (*i.e.*, $N_0 = 1.6 \times 10^4$; 8.0×10^4; 1.6×10^5; 3.2×10^5) as a function of cultivation time. All parameters used in this simulation are reported in Table 1. As it might have expected, by increasing $N_{0,}$ the cell number results augmented for each cultivation time considered. The time evolution of the total number of cell shows the typical oscillating behavior characterized by stationary periods followed by incremental steps. This fact depends on the time required for each stage

Table 1
Parameters for PB model used in the simulation.

Parameter	Value	Unit	References
N_0	$1.6 \times 10^4/3.2 \times 10^5$	Cells	Fadda et al. (2012b)
A_P	8.0×10^8	μm^2	Fadda et al. (2012b)
μ_v	1.37×10^3	μm^3	This work
σ_v	3.0×10^2	μm^3	This work
μ_ξ	0.2 or 0.5	–	This work
σ_ξ	0.01 or 0.15	–	This work
k_v	0.035	h^{-1}	Fadda et al. (2012b)
v_{min}	20.0	μm^3	Fadda et al. (2012b)
v_{max}	7000.0	μm^3	Fadda et al. (2012b)
α	1.6	–	Fadda et al. (2012b)
w	7.8	–	Fadda et al. (2012b)
λ	1.78×10^3	μm^3	Fadda et al. (2012b)
q	40	–	Mancuso et al. (2009)
r_ξ^{G1}	0.1842	h^{-1}	This work
r_ξ^{S}	0.0943	h^{-1}	This work
$r_\xi^{G2/M}$	0.125	h^{-1}	This work

of the cell cycle to undergo the transition to the next phase. Starting from cell synchronized in G1 phase (as imposed by the initial condition) a period of time is required for the cells to enter the next phase S, then another period of time to reach the G2/M stage and finally a further lag time for cell to undergo mitosis. By observing Fig. 6, it clearly appears that the proposed model

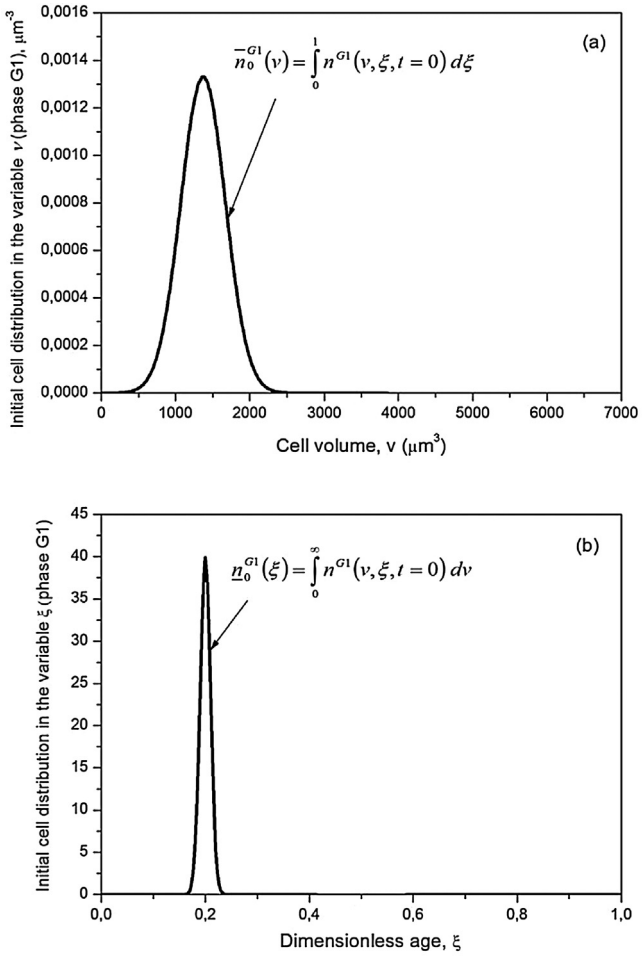

Fig. 5. Initial distribution of cells in phase G1 as a function of cell volume (a) and dimensionless age (b). Parameters of the bivariate gaussian function used to describe initial distribution are reported in Table 1 ($\mu_\xi = 0.2$ and $\sigma_\xi = 0.01$ in this simulation).

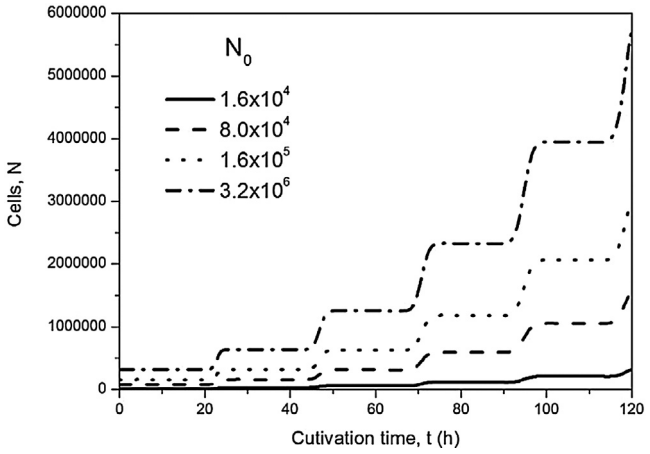

Fig. 6. Model results in terms of total cell count evolution versus cultivation time obtained at different initial seeding condition.

properly describes the well-known oscillating behavior of the cell cycle. In particular, it results that one complete cell cycle progression requires 24 h coherently with the time, in terms of age of maturation τ^{P}, determined by the adopted kinetic model. By means of this modeling approach, it is also possible to describe the characteristic "incubation/acclimation" time which may occur at the beginning of cultivation. Cells may undergo mitosis only if they reach the G2/M by experiencing the transition G2/M → G1. The latter one requires a period of time for cells which are initially synchronized in G1 phase. In the simulations depicted in Fig. 6, this incubation time corresponds to about 24 h, coherently with the time needed by cells starting in the stage G1 to complete the cell cycle. Fig. 7 shows model results in terms of cell count evolution for each cell cycle phase as a function of cultivation time obtained at different initial seeding condition (*i.e.*, $N_0 = 1.6 \times 10^4$, 8.0×10^4, 1.6×10^5 and 3.2×10^5 for Fig. 7a–d, respectively). To facilitate the comparison we kept the same *x*-axis scale for all figures. Cells belonging to phase G1, S and G2/M display a typical oscillating behavior going from a minimum value to a (relative) maximum one. Cells belonging to S stage appear after the maturation in G1 phase is completed. A decreasing in cell number of cell in G1 phase corresponds to an increasing number of cells in the subsequent phase S. The same aspect can be observed for the transition S → G2 M. When cells belonging to G2/M stage undergo mitosis the cell cycle restarts and new daughter cells appear in G1 phase. From Fig. 7, it is apparent that transitions occur coherently with the maturation age (*i.e.*, for G1 → S starts after $\tau^{G1} = 5.4$ h; S → G2/M occurs after other $\tau^{S} = 10.6$ h and finally G2/M→ takes places after $\tau^{G2/M} = 8$ h). The quiescent/senescent phase G0, consisting of cells which exit the cell cycle, leaving in particular the G1 stage (transition G1 → G0), displays an oscillating "step" behavior. Since in the present work the transition G0 → G1 is neglected (irreversible cell cycle exit), the total number of cell in the stage G0 cannot decrease, as coherently obtained by the model results. Cell can enter (irreversibly) the G0 stage, as properly described by the proposed model, on the basis of the contact inhibition effect, which becomes important as the total cell number increases (less available space for cell growth). Therefore, by increasing the initial cells number seeded on Petri dish one can expect a higher rate of cell entering the G0 phase, as properly simulated by the model results shown in Fig. 7. From the latter ones, it is also worth noting, that the rate of cells entering

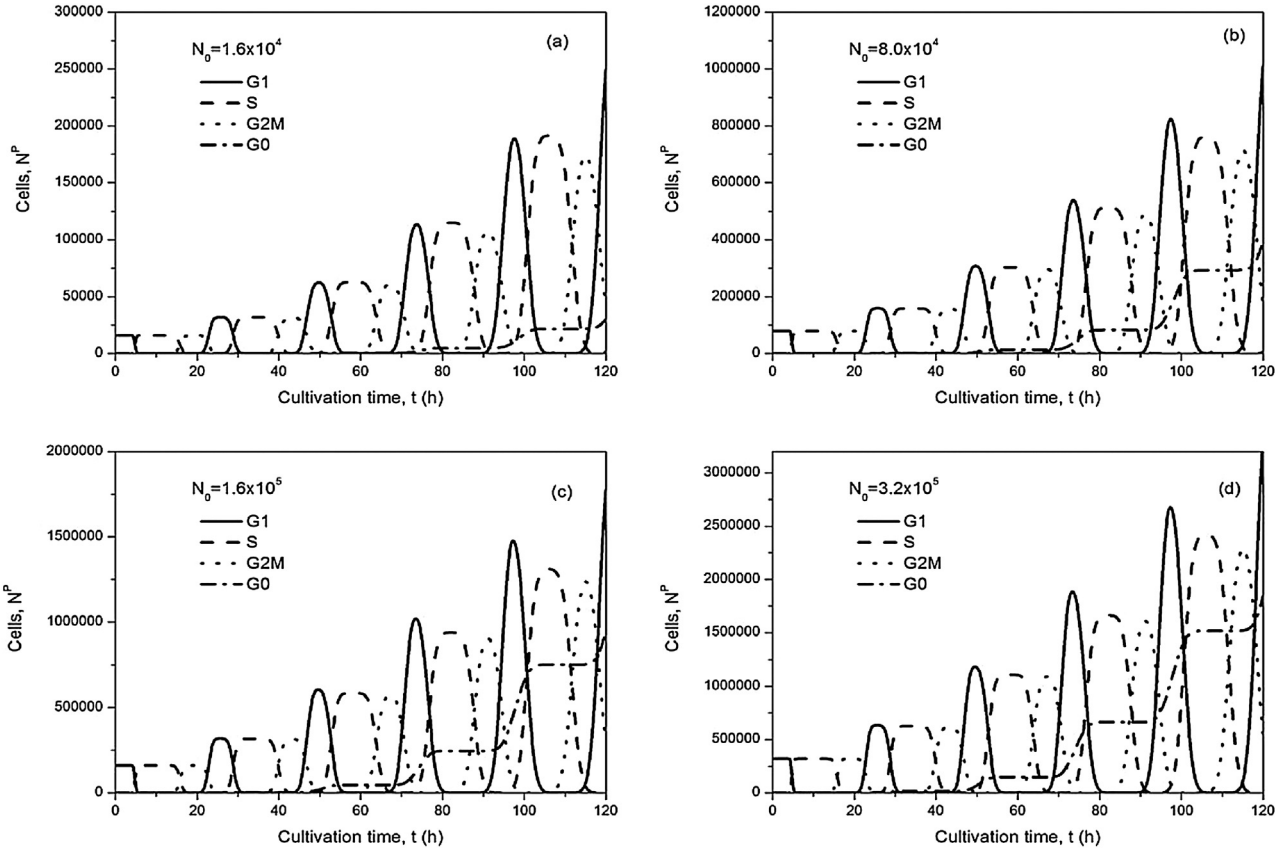

Fig. 7. Model results in terms of cell count evolution for each cell cycle phase versus cultivation time obtained at different initial seeding condition: (a) $N_0 = 1.6 \times 10^4$; (b) $N_0 = 8.0 \times 10^4$; (c) $N_0 = 1.6 \times 10^5$; and (d) $N_0 = 3.2 \times 10^5$.

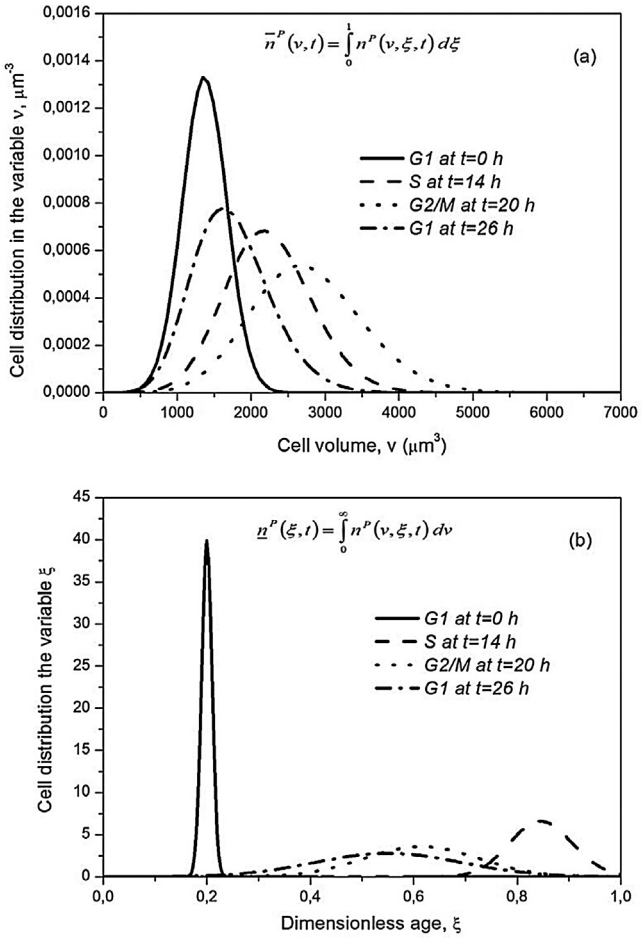

Fig. 8. Cell distribution as a function of cell volume (a) and dimensionless age (b) at various cultivation time (*i.e.*, $t = 0, 14, 20, 26$ h) for cells belonging to G1, S and G2/M phase for the case when $N_0 = 1.6 \times 10^5$.

G0 phase approaches zero (constant value of cell number in G0 stage) when cells belonging to G1 phase end the transition to the subsequent active phase S. This fact is correctly described by the proposed model as clearly illustrated in Fig. 7. Consequently, the increasing of cell number in G0 phase starts to stop. Initial distribution of cells in phase G1 as a function of cell volume and dimensionless age, for various cultivation time, are shown in Fig. 8 where the case of seeding with $N_0 = 1.6 \times 10^5$ is considered. Cells at $t = 0$ belong to G1 phase while at $t = 14$ h the transition G1 → S is already completed ($t > \tau^{G1}$) and cells are in S state displaying volume distribution with an higher *moda* value, with respect to the one at $t = 0$, since cell volume at 14 h is obviously increased (Fig. 8a). Similarly, at $t = 20$ h, after the transition S → G2/M, cells belong to G2/M phase with a *moda* distribution which shows an higher value with respect to the previous one for phase S at $t = 14$ h. Finally, when cells undergo mitosis, new (and smaller) daughter cells appear in G1 phase ($t = 26$ h) and their volume distribution displays a lower value of *moda* with respect to the one shown at $t = 20$ h for cells belonging to G2/M phase. In Fig. 8b the same behavior is illustrated in terms of dimensionless age distribution. Increasing the cultivation time cell distribution curve displays an enlargement (cells with distribution of age spread over the entire range). Some hours after the cell cycle completion, at $t = 26$ h, cells belong again to the G1 phase with a *moda* distribution that displays a lower value with respect to the ones defined at lower time (*i.e.*, $t = 14$ h in S phase, $t = 20$ h in G2/M phase).

The proposed model is also capable to simulate smoothed oscillating behavior which may take place as a result of the specific conditions adopted. To this aim we can consider the following bivariate normal Gaussian function to describe the cell distribution at $t = 0$, used in initial conditions (5), (7), and (8), for cells belonging to the phase P = G1, S, and G2/M, respectively:

$$n_0^P(v,\xi) = \frac{(N_0/3)}{2\pi\sigma_v\sigma_\xi}\exp\left(-\frac{1}{2}\left[\frac{(v-\mu_v)^2}{\sigma_v^2} + \frac{\left(\xi-\mu_\xi\right)^2}{\sigma_\xi^2}\right]\right)$$

Parameters of the bivariate gaussian function are reported in Table 1 ($\mu_\xi = 0.5$ and $\sigma_\xi = 0.15$) while the initial distribution of cells in G1, S, G2/M as a function of v and ξ are shown in Fig. 9. The effect of the seeding conditions is illustrated in Fig. 10 where model results are reported in terms of total cell count evolution as a function of cultivation time for an initial cell number $N_0 = 1.6 \times 10^5$. Solid line represents the simulation result when cells are seeded at G1-phase (parameters of simulation reported in Table 1 for the case when $\mu_\xi = 0.2$ and $\sigma_\xi = 0.01$) while the dashed line is related to the situation where the seeded cells belonging to all active phases, *i.e.*, G1, S, G2/M (parameters of simulation reported in Table 1 with $\mu_\xi = 0.5$ and $\sigma_\xi = 0.15$) start being cultivated.

By observing Fig. 10, it is apparent that the temporal behavior represented by the dashed line displays a smoother trend if

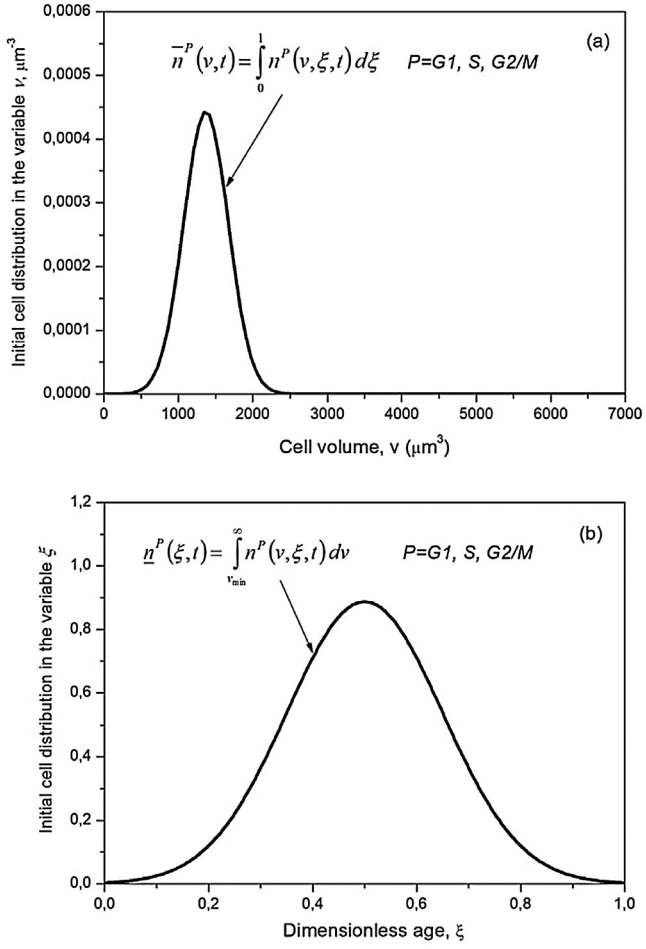

Fig. 9. Initial distribution of cells in phase P = G1, S and G2/M as a function of cell volume (a) and dimensionless age (b). Parameters of the bivariate gaussian function, used to describe initial distribution, are reported in Table 1 ($\mu_\xi = 0.5$ and $\sigma_\xi = 0.15$ in this simulation).

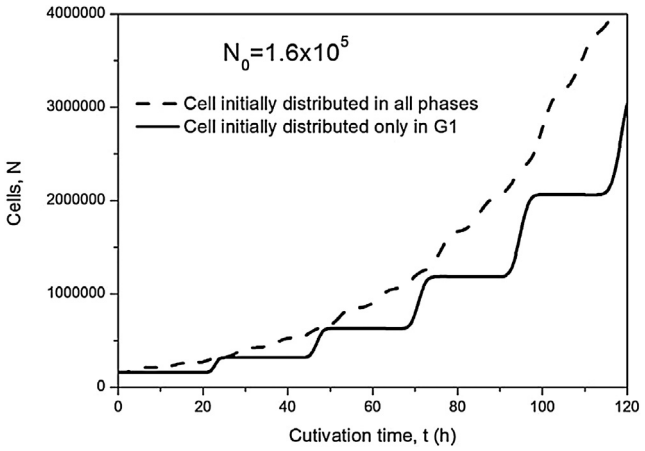

Fig. 10. Model results in terms of total cells count evolution versus cultivation time obtained at different initial cell distribution in terms of age and progression phase. Solid line represents the simulation result when seeded cells start cultivation belonging to the G1-phase; dashed line represents the simulation result when seeded cells start cultivation belonging to all active phases, *i.e.*, G1, S, G2/M.

compared with the one depicted with the solid line. Indeed, in the case represented by the dashed line, at $t = 0$ cells are distributed in all active phases (G1, S and G2/M) thus cells belonging to G2/M can undergo mitosis after few minutes, thus increasing the total number of cell even at the beginning of the cultivation. Cells in G1 stage can enter the subsequent phase S, and those ones belonging to the S one can proceed to the G2/M phase by ensuring a sort of continuous behavior in the cell expansion. On the other hand, with a lag time of about 24 h (the typical cell time for one cell cycle completion) the solid line "reaches" the dashed one, since cells, initially synchronized only in G1 phase, have experienced all cell cycle. In Fig. 10, it is also possible to note that the difference between the two temporal profile increases as the cultivation time augments.

Finally, model results in terms of total cell count evolution as a function of cultivation time for the base case (cell cycle completed in 24 h, solid line) are compared in Fig. 11 to those ones obtained by simulating the use of a cytostatic drug (cell cycle completed in 30 h, dot-dashed line) or a substance acting as a growth factor during cell proliferation (cell cycle completed in 17 h, dot-dashed line). All model parameters used in simulations are reported in

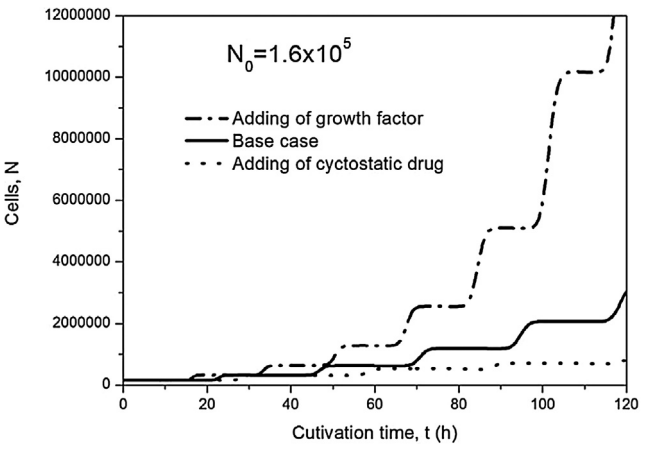

Fig. 11. Model results in terms of total cell count evolution versus cultivation time for the base case (cell cycle completed in 24 h, solid line), computed to the case where the use of a substance acting as a growth factor during cell proliferation (cell cycle completed in 17 h, dot-dashed line) or a cytostatic drug (cell cycle completed in 30 h, dot-dashed line) is taken into account.

Table 1 except for $r_{\xi}^{G1} = 1/\tau^{G1} = 1/9.5\text{h} = 0.1053\text{h}^{-1}$, $r_{\xi}^{S} = 1/\tau^{S} = 1/10.5\text{h} = 0.0952\text{h}^{-1}$ and $r_{\xi}^{G2/M} = 1/\tau^{G2/M} = 1/10\text{h} = 0.1\text{h}^{-1}$, when a cytostatic drug is added during the culture cultivation (cell cycle time for phase transition as shown in Fig. 4b) and $r_{\xi}^{G1} = 1/\tau^{G1} = 1/2.6\text{h} = 0.3846\text{h}^{-1}$, $r_{\xi}^{S} = 1/\tau^{S} = 1/4\text{h} = 0.25\text{h}^{-1}$ and $r_{\xi}^{G2/M} = 1/\tau^{G2/M} = 1/10.4\text{h} = 0.0961\text{h}^{-1}$ $r_{\xi}^{G2/M} = 1/\tau^{G2/M} = 1/10.4\text{h} = 0.0961\text{h}^{-1}$ when a substance to inhibits the synthesis of pRB protein is used (cell cycle time for phase transition as shown in Fig. 4c). From a view inspection of Fig. 11 the cytostatic effect of the drug, which results in a slowdown of the cell cycle progression (30 h are needed to complete an entire cycle instead of 24 h as in the base case), is apparent. On the other hand, the positive contribution in terms of cell proliferation of a substance which acts on pRB rate of synthesis by leading to a shortening of cell cycle duration (17 h instead of 24 h as in the base case) may be clearly seen. The coupling of a comprehensive biochemical model with a multistage population balance, as clearly demonstrated by the results reported in Fig. 11, shows that the proposed approach represents a powerful tool to predict the effect of specific chemical species on the temporal evolution of the cell cycle. The proposed model, in the light of simulations discussed in this work, presents versatile features which appear undoubtedly useful for description of *in vitro* cell proliferation processes.

4. Concluding remarks

In this work, a novel mathematical model helpful to investigate cell proliferation kinetics is developed. Specifically, the model is based on a PB approach that allows one to quantitatively describe cell cycle progression through the different phases experienced by all the cells of the entire population during their own life. The transitions between two consecutive cell cycle phases are governed by a complex network of biochemical kinetics related to mammalian cells and proposed by Gérard and Goldbeter (2009), which involves CDKs and their association with cyclins and protein inhibitors, phosphorylation–dephosphorylation, and cyclin synthesis or degradation. Time of each phase duration, required by the 2D multi-staged PB developed in this work, is estimated by considering the evolution of biochemical reactions until check point for transition is reached. Specific examples are discussed to illustrate the ability of the proposed model to simulate the effect of drug and growth factors during *in vitro* cell cultivation for applications in oncology, medicine regenerative or tissue engineering. The coupling proposed in this work of a detailed biochemical model with a multistage population balance represents therefore an useful and powerful tool to simulate the effect on the cell proliferation due to substances/drugs that can accelerate or decelerate the cell cycle. The model also properly accounts for the variation of cell volume during cell growth and proliferation which can be helpful for model validation by direct comparison with experimental data where the cell size distribution can be suitably provided. A possible future work direction may be addressed toward a more rigorous description of the cell size growth in connection with its metabolism and by accounting for the not negligible cell-to-cell interactions.

Acknowledgement

This work has been carried out with the financial contribution of the Sardinian Regional Authorities (SICELLS Project).

References

Aguda, B.D., Tang, Y., 1999. The kinetic origins of the restriction point in the mammalian cell cycle. Cell Prolif. 32, 321–335.

Bouchoux, C., Uhlmann, F., 2011. A quantitative model for ordered Cdk substrate dephosphorylation during mitotic exit. Cell 147, 803–814.

Chen, K.C., Csikasz-Nagy, A., Gyorffy, B., Val, J., Novak, B., Tyson, J.J., 2000. Kinetic analysis of a molecular model of the budding yeast cell cycle. Mol. Biol. Cell 11, 369–391.

Chen, K.C., Calzone, L., Csikasz-Nagy, A., Cross, F.R., Novak, B., Tyson, J.J., 2004. Integrative analysis of cell cycle control in budding yeast. Mol. Biol. Cell 15, 3841–3862.

Ciliberto, A., Novak, B., Tyson, J.J., 2003. Mathematical model of the morphogenesis checkpoint in budding yeast. J. Cell Biol. 163, 1243–1254.

Cooper, G.M., 1997. The Cell: A Molecular Approach. ASM Press, Herdorn.

Csikasz-Nagy, A., Battogtokh, D., Chen, K.C., Novak, B., Tyson, J.J., 2006. Analysis of a generic model of eukaryotic cell-cycle regulation. Biophys. J. 90, 4361–4379.

Fadda, S., Cincotti, A., Cao, G., 2012a. A novel population balance model to investigate the kinetics of in vitro cell proliferation: part I. Model development. Biotechnol. Bioeng. 109, 772–781.

Fadda, S., Cincotti, A., Cao, G., 2012b. A novel population balance model to investigate kinetics of in vitro cell proliferation: part II. Numerical solution parameters' determination and model outcomes. Biotechnol. Bioeng. 109, 782–796.

Faraday, D.B.F., Hayter, P., Kirkby, N.F., 2001. A mathematical model of the cell cycle of a hybridoma cell line. Biochem. Eng. J. 7, 49–68.

Florian, J.A., Parker, R.S., 2005. A population balance model of cell cycle-specific tumor growth. Proceedings of the 16th IFAC World Congress, Praga.

Fredrickson, A.G., Mantzaris, N.V., 2002. A new set of population balance equations for microbial and cell cultures. Chem. Eng. Sci. 57, 2265–2278.

Gérard, C., Goldbeter, A., 2009. Temporal self-organization of the cyclin/Cdk network. PNAS 106, 21643–21648.

Gérard, C., Goldbeter, A., 2012. From quiescence to proliferation: Cdk oscillations drive the mammalian cell cycle. Front. Physiol. 3 (A413), 1–18.

Hatzis, C., Srienc, F., Fredrickson, A.G., 1995. Multistaged corpuscolar models of microbial growth: Monte Carlo simulations. Biosystems 36, 19–35.

Himmelblau, F.M., Bischoff, K.B., 1968. Process Analysis and Simulation: Deterministic Systems. Wiley, New York.

Hochegger, H., Takeda, S., Hunt, T., 2008. Cyclin-dependent kinases and cell-cycle transitions: does one fit all? Nat. Rev. Mol. Cell Biol. 9, 910–916.

Horch, R.E., 2006. Future perspectives in tissue engineering. J. Cell. Mol. Med. 10, 4–6.

Karra, S., Sager, B., Karim, M.M., 2010. Multi-scale modeling of heterogeneities in mammalian cell culture processes. Ind. Eng. Chem. Res. 49, 7990–8006.

Lanza, R., Langer, R., Vacanti, J., 1996. Principles of Tissue Engineering. Academic Press Inc., San Diego.

Liou, J.J., Srienc, F., Fredrickson, A.G., 1997. Solutions of population balance models based on a successive generations approach. Chem. Eng. Sci. 52, 1529–1540.

Liu, Y.H., Bi, J.X., Zeng, A.P., Yuan, J.Q., 2007. A population balance model describing the cell cycle dynamics of myeloma cell cultivation. Biotechnol. Prog. 23, 1198–1209.

Loog, M., Morgan, D.O., 2005. Cyclin specificity in the phosphorylation of cyclindependent kinase substrates. Nature 434, 104–108.

Mancuso, L., Liuzzo, M.I., Fadda, S., Pisu, M., Cincotti, A., Arras, M., Desogus, E., Piras, F., Piga, G., La Nasa, G., Concas, A., Cao, G., 2009. Experimental analysis and modeling of in vitro mesenchymal stem cells proliferation. Cell Prolif. 42, 602–616.

Mancuso, L., Liuzzo, M.I., Fadda, S., Pisu, M., Cincotti, A., Arras, M., La Nasa, G., Concas, A., Cao, G., 2010. In vitro ovine articular chondrocyte proliferation: experiments and modeling. Cell Prolif. 43, 310–320.

Mantzaris, N.V., Liou, J.J., Daoutidis, P., Srienc, F., 1999. Numerical solution of a mass structured cell population balance in an environment of changing substrate concentration. J. Biotechnol. 71, 157–174.

Morgan, D.O., 1995. Principles of Cdk regulation. Nature 374, 131–134.

Morgan, D.O., 1997. Cyclin-dependent kinases: engines, clocks, and microprocessors. Annu. Rev. Cell Dev. Biol. 13, 261–291.

Morgan, D.O., 2007. The Cell Cycle: Principles of Control, second ed. New Science Press, London.

Novak, B., Tyson, J.J., 2004. A model for restriction point control of the mammalian cell cycle. J. Theor. Biol. 230, 563–579.

Nurse, P., 2000. A long twentieth century of cell cycle and beyond. Cell 100, 71–78.

Pisu, M., Lai, N., Cincotti, A., Delogu, F., Cao, G., 2003. A simulation model for the growth of engineered cartilage on polymeric scaffolds. Int. J. Chem. React. Eng.. http://www.bepress.com/ijcre/vol1/A38.

Pisu, M., Lai, N., Cincotti, A., Concas, A., Cao, G., 2004. Model of engineered cartilage growth in rotating bioreactors. Chem. Eng. Sci. 59, 5035–5040.

Pisu, M., Concas, A., Lai, N., Cao, G., 2006. A novel simulation model for engineered cartilage growth in static systems. Tissue Eng. 12, 2311–2320.

Pisu, M., Concas, A., Cao, G., 2007. A novel simulation model for stem cells differentiation. J. Biotechnol. 130, 171–182.

Pisu, M., Concas, A., Fadda, S., Cincotti, A., Cao, G., 2008. A simulation model for stem cells differentiation into specialized cells of non-connective tissues. Comput. Biol. Chem. 32, 338–344.

Popović, M.K., Pörtner, R., 2012. Bioreactors and cultivation systems for cell and tissue culture. In: Doelle, H.W., Rokem, S., Berovic, M. (Eds.), Encyclopedia of Life Support Systems (EOLLS). Eolss Publishers, Oxford.

Qu, Z., Weiss, J.N., MacLellan, W.R., 2003. Regulation of the mammalian cell cycle: a model of the G1-to-S transition. Am. J. Physiol. 284, C349–C364.

Ramkrishna, D., 2000. Population balances. Theory and Applications to Particulate Systems in Engineering. Academic Press Inc., San Diego.

Schiesser, W.E., 1991. The Numerical Method of Lines. Academic Press, San Diego.

Shapiro, G.I., Harper, W., 1999. Anticancer drug targets: cell cycle and checkpoint control. J. Clin. Investig. 104, 645–1653.

Sherer, E., Tocce, E., Hannemann, R.E., Rundell, A.E., Ramkrishna, D., 2008. Identification of age-structured models: cell cycle phase transitions. Biotechnol. Bioeng. 99, 960–974.

Sidoli, F.R., Aspery, S.P., Mantalaris, A., 2006. A coupled single cell-population model for mammalian cell cultures. Ind. Eng. Chem. Res. 45, 5801–5811.

Stern, B., Nurse, P., 1996. A quantitative model for cdc2 control of S phase and mitosis in fission yeast. Trends Genet. 12, 345–350.

Tyers, M., 2004. Cell cycle goes global. Curr. Opin. Cell Biol. 16, 602–613.

Tyson, J.J., 1991. Modeling the cell-division cycle – Cdc2 and cyclin interactions. Proc. Natl. Acad. Sci. U. S. A. 88, 7328–7332.

Tzur, A., Kafri, R., LeBleu, V.S., Lahav, G., Kirschner, M.W., 2009. Cell growth and size homeostasis in proliferating animal cells. Science 325, 167–171.

Wittemberg, C., 2012. A division duet. Nature 481, 273–274.